Swiss J Geosci (2017) 110:777–791
DOI 10.1007/s00015-017-0277-0

Biostratigraphy and seismic data analysis to detect the sequence stratigraphic depositional environment of the Miocene succession: Gulf of Suez (Egypt)

Ahmed Abd El Naby[1] · Wafaa Abd-Elaziz[2] · Mohamed Hamed Abdel Aal[2]

Received: 22 November 2016 / Accepted: 9 June 2017 / Published online: 26 June 2017

Abstract This work comprises a study of the sequence stratigraphy, seismic-facies analysis, biostratigraphy and depositional environments of the northern part of the Gulf of Suez, Egypt, using a set of 24 3D seismic profiles, composite logs and sonic logs from ten wells. The syn-rift formations in the studied ten wells are described lithologically and interpreted based on investigating two seismic profiles. Biostratigraphically, the Miocene fossils are identified to correlate the five planktonic foraminiferal biozones in the examined boreholes (RB-A1, RB-B1, RB-B3, EE85-2 and RB-C1). The sequence stratigraphic analysis suggests that the Miocene succession can be subdivided into two major third order depositional sequences (S1 and S2) separated by the three major sequence boundaries (DSB1, DSB2 and DSB3).

Keywords Miocene · Tectonic structure · Sequence stratigraphy · Seismic facies · Biostratigraphy · Gulf of Suez · Egypt

Editorial handling: W. Winkler.

✉ Ahmed Abd El Naby
zowail2000@yahoo.com

Wafaa Abd-Elaziz
wafaa_a_ali@yahoo.com

Mohamed Hamed Abdel Aal
mabdelaal81@yahoo.com

[1] Department of Geology, Faculty of Science, Ain Shams University, Cairo, Egypt

[2] Department of Biological and Geological Science, Faculty of Education, Ain Shams University, Cairo, Egypt

1 Introduction

The Gulf of Suez covers an area of about 25,000 km^2. It extends from latitude 27° 30′N to 30° 00′N as a northwest-elongated structural depression at the northern end of the Red Sea. It is 350 km long, while its width varies from 52 km in the north to 90 km in the south. Both the eastern and western coastal belts exhibit a sedimentary sequence that extends offshore. The Gulf of Suez is a rather shallow and narrow body of water. Its average depth does not exceed 55 m. Several islands, formed by emerging fault blocks, are present near its junction with the Red Sea. The gulf itself is bordered by a similarly structured coastal belt. The proven overall onshore and offshore oil potential is distributed within about 38,500 km^2 (Schlumberger 1984).

The study area is located in the northern part of the Gulf of Suez (Belayim offshore concession area), approximately 4 km from the east coast of Gulf of Suez and 13 km northwest of Abu Rudeis, at a water depth of approximately 43 m. It is restricted between latitudes 29° 00′ and 28° 50′N and between longitudes 32° 50′ and 33° 10′E (Fig. 1). The objective of this paper is to investigate the nature of the geologic events (biostratigraphy and facies changes), and hence interpret the sequence stratigraphy of the syn-rift rocks in the northern part of the Gulf of Suez and their impact on hydrocarbon exploration.

2 Geologic setting

The Gulf of Suez structure is affected by a complicated fault patterns: NW clysmic faults, E–W and N–S to NNE–SSW trending normal faults (Garfunkel and Bartov 1977; Colletta et al. 1988; Moustafa 1993; Bosworth 1995;

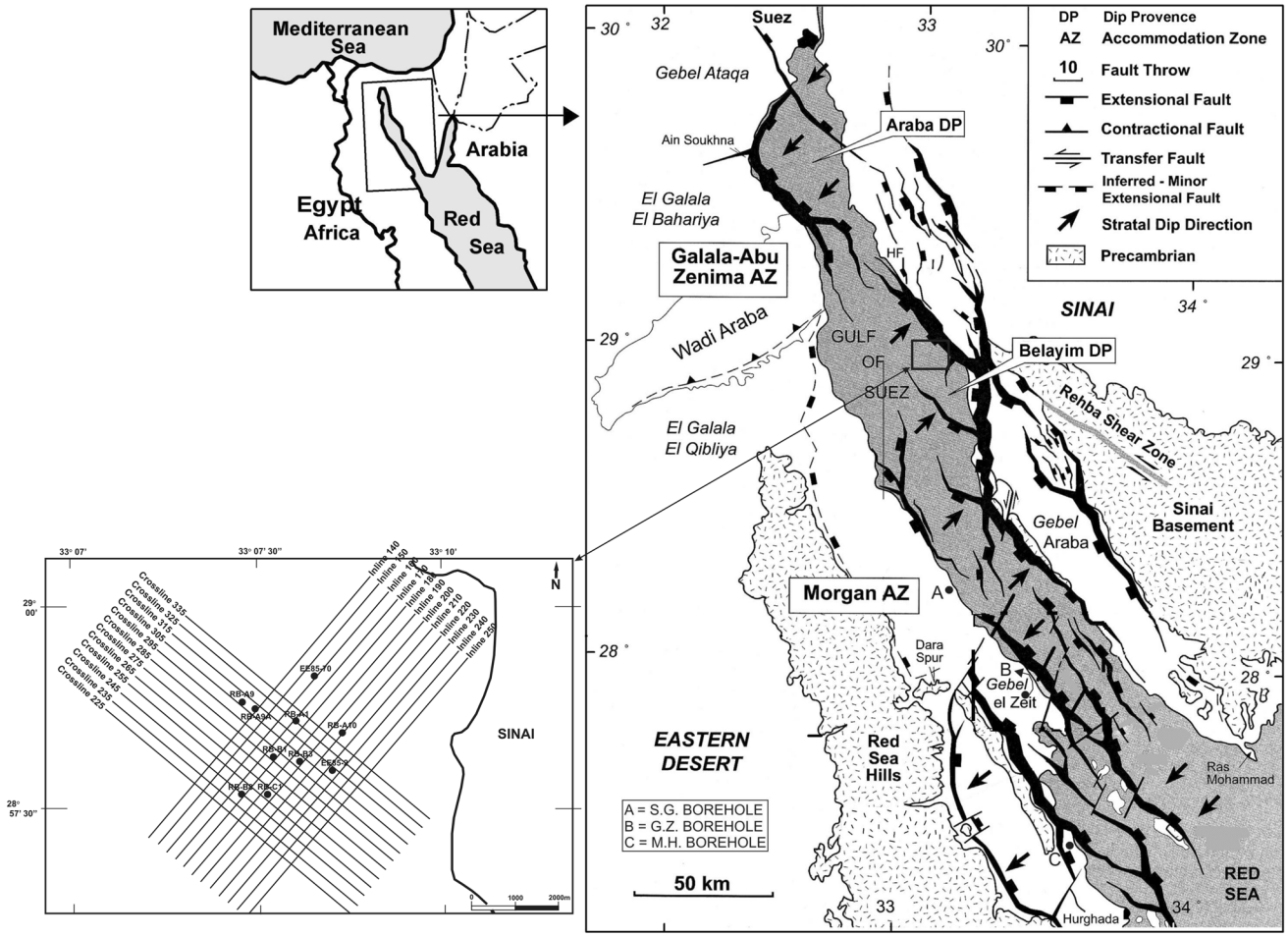

Fig. 1 Tectonic map of the Gulf of Suez Rift modified after Bosworth and McClay (2001). The study area (*rectangle*, including location of the wells) is located in the Belayim dip province

McClay et al. 1998). There are also NE trending strike-slip faults crossing the gulf basin.

The extension of the Gulf of Suez rift basin was interpreted as a result of the interaction of the four major fault trends during the Late Oligocene-Early Miocene. Three of these trends are the Clysmic trend, North-oblique faults trend and Northwest-oblique faults trend (Patton et al. 1994). The fourth trend faults are oriented between 50° and 75° azimuth and have been referred to as cross faults perpendicular to the clysmic trend. Both oblique left-lateral and oblique right-lateral strike-slip motions have been recorded for the cross-trending faults (Younes and McClay 2002). According to their structural setting and regional dip direction, the Gulf of Suez is subdivided into three structural provinces. These three structural provinces are separated from each other by two NNE-SSW hinge zones: the Galala-Abu Zenima Accommodation zone in the north, and the Morgan Accommodation zone in the south (Fig. 1, Patton et al. 1994). These provinces, from north to south are the northern Araba dip province (SW dips), the central Belayim dip province (NE dips), and the southern Amal-Zeit dip province (SW dips, Fig. 1). The study area is located in the central Belayim dip province (Fig. 1).

The Miocene successions of the study area as derived from drill holes data (Fig. 2) consists of syn-rift sediments representing important source, reservoir and seal rocks that unconformably overlie the Eocene Thebes Formation. They range in age from Oligocene (Abu Zenima red beds) and syn-rift volcanics to Miocene (Nukhul, Rudeis, Kareem, Belayim, South Gharib and Zeit Formations), and post-rift units that is represented by Pliocene-Recent post-Zeit rocks. This phase closes the depositional history of the Suez graben area (Schlumberger 1995).

3 Description of Syn-rift sediments

The syn-rift formations as exhibited in the seismic profiles Crossline 315 and Inline 200 (Figs. 1, 3, 4) are distributed along the offshore northern part of the Gulf of Suez region.

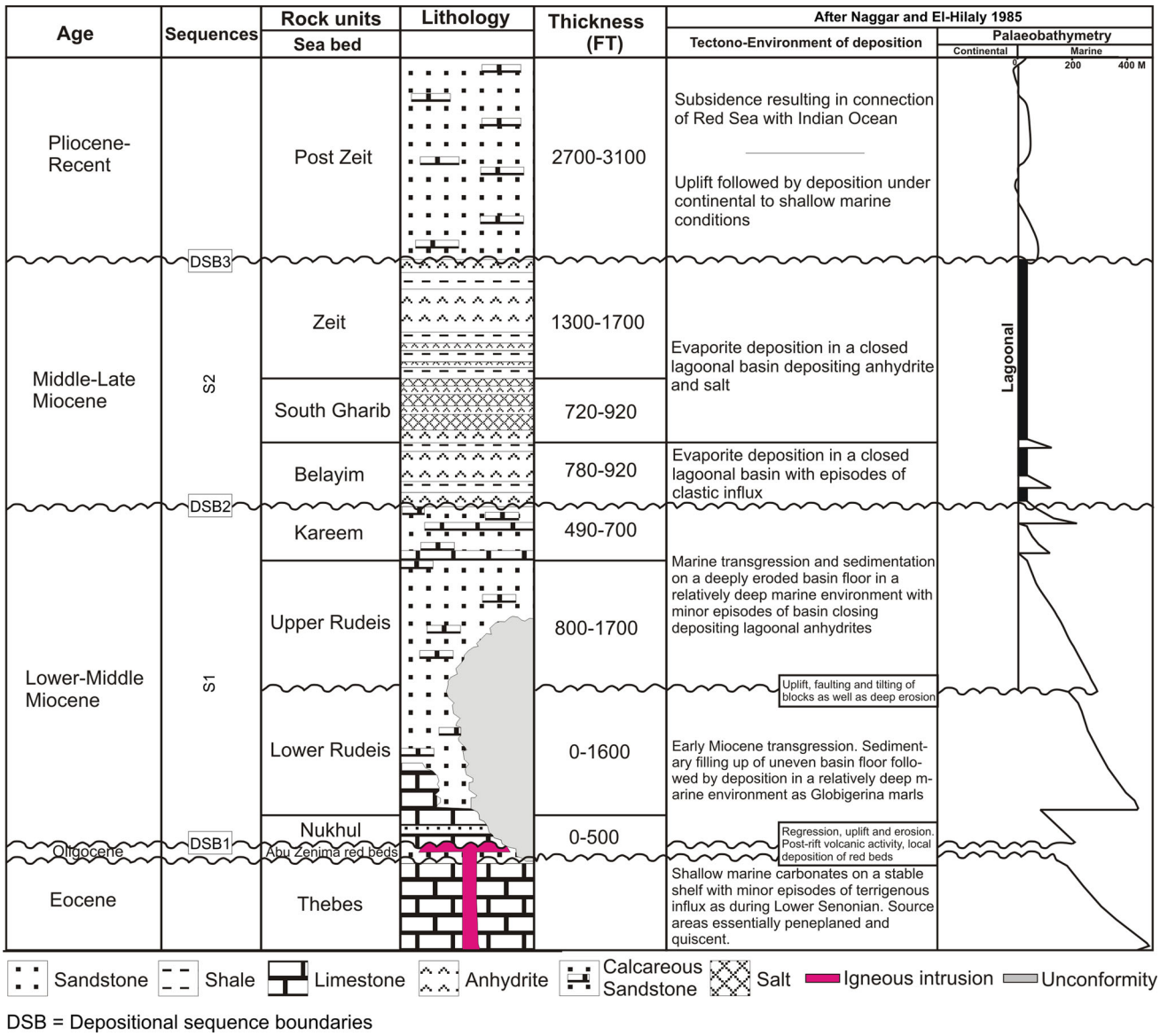

Fig. 2 Generalised stratigraphic column of the Miocene succession shows the tectonic environment of deposition and palaeobathymetry of the northern part of the Gulf of Suez (modified after Naggar and El-Hilaly 1985)

Six lithostratigraphic units are distinguished. From base to top, they are: Nukhul, Rudeis, Kareem, Belayim, South Gharib and Zeit formations (Figs. 3, 4, 5, 6, 7).

3.1 The Nukhul Formation

The Nukhul Formation is recorded only in three wells (RB-A1, EE85-2 and RB-C1), while it is missing in two other wells (RB-B1and RB-B3) as shown in Figs. 1, 5, 6, 7. This formation is also not recorded on the seismic profiles due to poor processing (Figs. 3, 4, 8, 9, 10, 11). The Aquitanian-Early Burdigalian Nukhul Formation is composed of sandstones, limestones and marls, reflecting the first marine syn-rift sequence in the Gulf of Suez. Its type section is in Wadi Nukhul (Scott and Govean 1985; Bosworth and McClay 2001). In the study area this formation unconformably overlies the Abu Zenima red beds (Fig. 2). The Nukhul Formation comprises also chert clasts of Eocene and Late Cretaceous origin and basement-derived basalt, indicating extensive early rift erosion during the deposition of this formation (Bosworth and McClay 2001). The base of this formation coincides with the lower depositional sequence boundary (DSB1) of the lower depositional sequence (Figs. 2, 5, 6, 7, see Sect. 5 for more discussion).

3.2 The Rudeis Formation

The Rudeis Formation consists mainly of shales, argillaceous limestones, calcareous shales and marls (Figs. 3, 4, 5, 6, 7) deposited in deeper marine environment

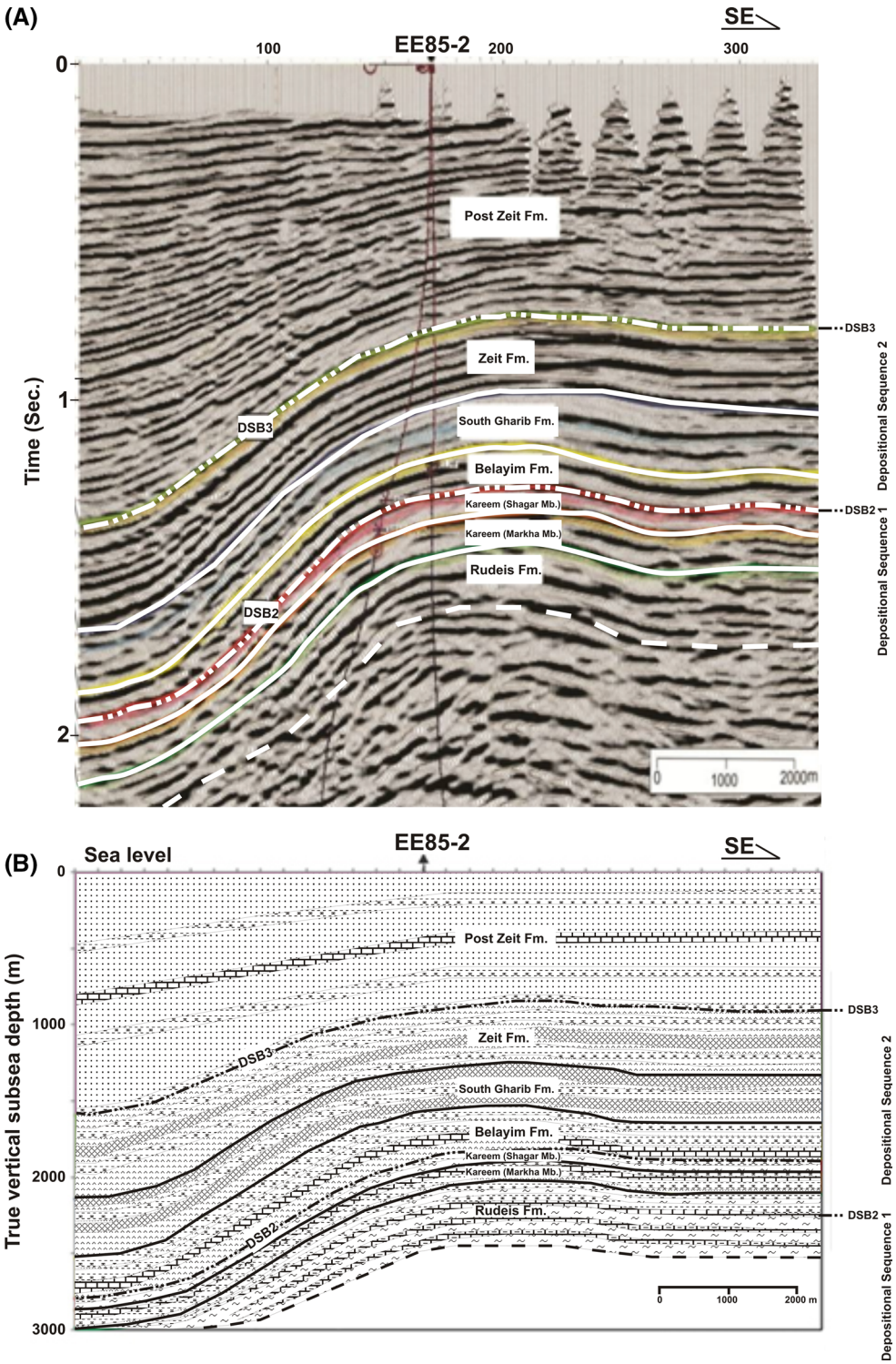

Fig. 3 **a** Interpreted seismic section Crossline 315, passing through the Middle part of the study area and running NW–SE direction (Fig. 1). This section illustrates the two depositional sequences and their bounding sequence boundaries (DSB2 and DSB3). The lower sequence boundary (DSB1) is not recorded due to poor processing. **b** Geologic interpretation of the seismic section Crossline 315 reveals the different lithologic facies of the Miocene units of the two depositional sequences (for legend see Fig. 5)

(Richardson and Arthur 1988). The thickness of this formation varies from 689 m at well EE85-2 to 229 m at well RB-B1 (Fig. 7). The Rudeis Formation is subdivided into Lower Rudeis and Upper Rudeis units (Bosworth and McClay 2001). The Lower Rudeis Member consists of argillaceous limestones, calcareous shales and marls and its thickness changes from 215 m at well A1 to 400 m at well EE85-2 (Figs. 5, 6, 7). It is eroded towards the central part of the study area at wells (RB-B1 and RB-B3, Figs. 5, 6, 7) contemporaneous with the beginning of significant rift shoulder uplift at 22 ± 1 Ma (Omar et al. 1989). The Rudeis Formation is unconformably underlain by the

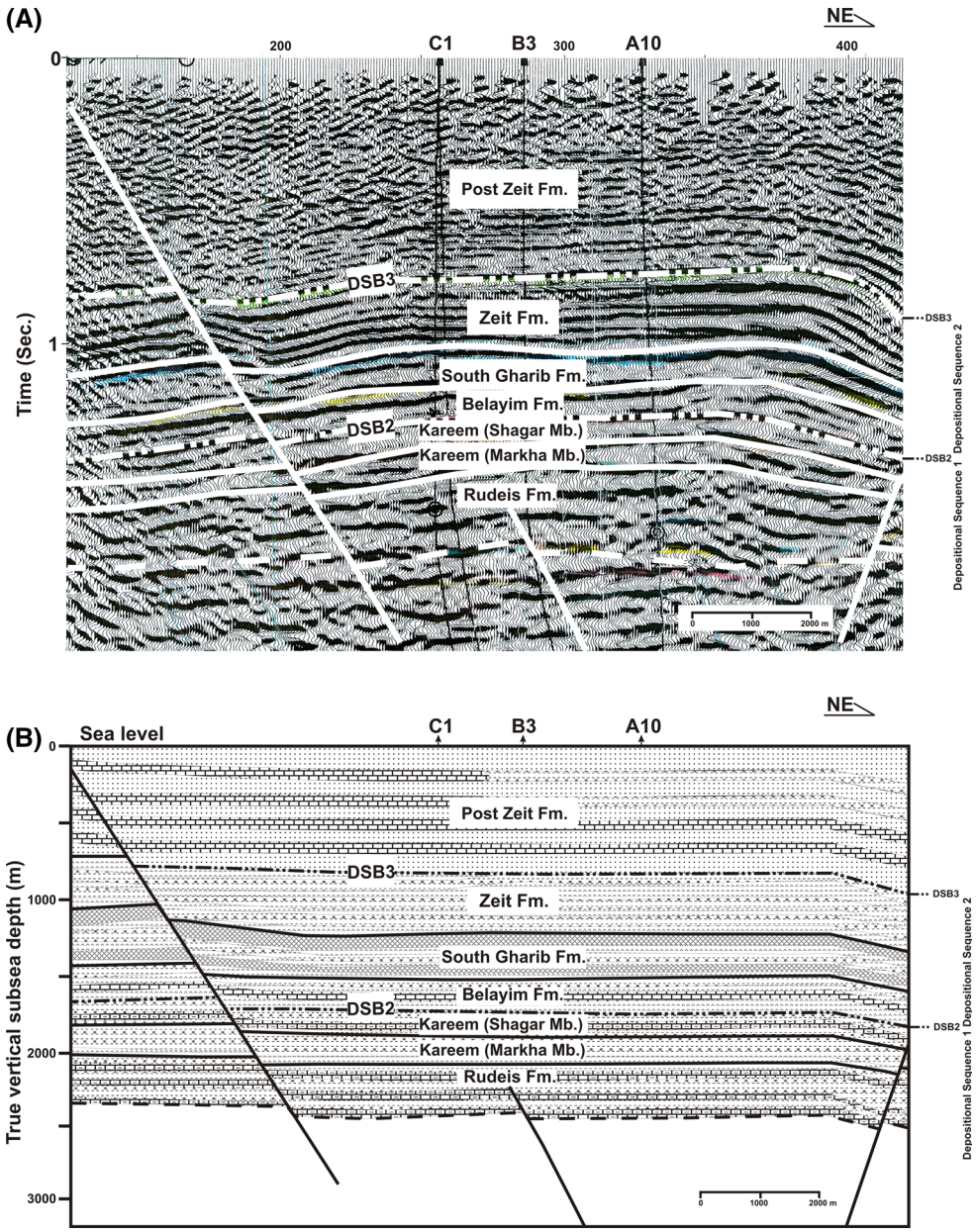

Fig. 4 **a** Interpreted seismic section Inline 200, passing through the middle part of the study area and running NE-SW direction (Fig. 1). This section shows two cross normal step faults in the SW (dipping towards the NE) and another cross fault in the NE (dipping towards SW) in the form of graben. Like Crossline 315, it also shows the two depositional sequences and their bounding sequence boundaries (DSB2 and DSB3), while the lower sequence boundary (DSB1) is also not recorded due to poor processing. **b** Geologic interpretation of the seismic section Inline 200 shows the different lithologic facies of the Miocene units of the two depositional sequences. This Inline denotes also the lithofacies changes of the post-Zeit Formation from mainly sandstones and limestones at the SW to mainly sandstones, limestones and calcareous shales at the NE (for legend see Fig. 5)

Eocene Thebes Formation at the central part of the study area at wells and conformably overlain by the Kareem Formation (Figs. 5, 6, 7) and is dated as early Burdigalian. The base of this formation cannot be followed on the seismic profiles due to poor processing (Figs. 3, 4). The deposition of the Lower Rudeis Member is followed by faulting, uplifting, tilting and deep erosion as well as regional and rapid subsidence of the Gulf of Suez basin referred to the "mid-clysmic" or "mid-Rudeis" event during which basin asymmetries (including transfer-accommodation-zones) in the rift basin were formed (Patton et al. 1994). Uneven topography created during intra-Rudeis erosional unconformity was filled in by sediments of the overlying Upper Rudeis Member (Naggar and El-Hilaly 1985). This member consists of shales, argillaceous limestones, calcareous shales and marls and its thickness varies from 289 m at well EE85-2 to 666 m at well RB-C1 (Figs. 5, 6, 7).

3.3 The Kareem formation

The Middle Miocene (Late Langhian/Early Serravallian, Ouda and Masoud 1993) Kareem Formation is composed mainly of calcareous shales, argillaceous limestones and marls with few anhydrites at the base (Figs. 3, 4, 5, 6, 7). The thickness of this formation varies from 149 m in well RB-A1 to 216 m in well EE85-2 and it unconformably overlies the Rudeis and underlies Belayim Formation

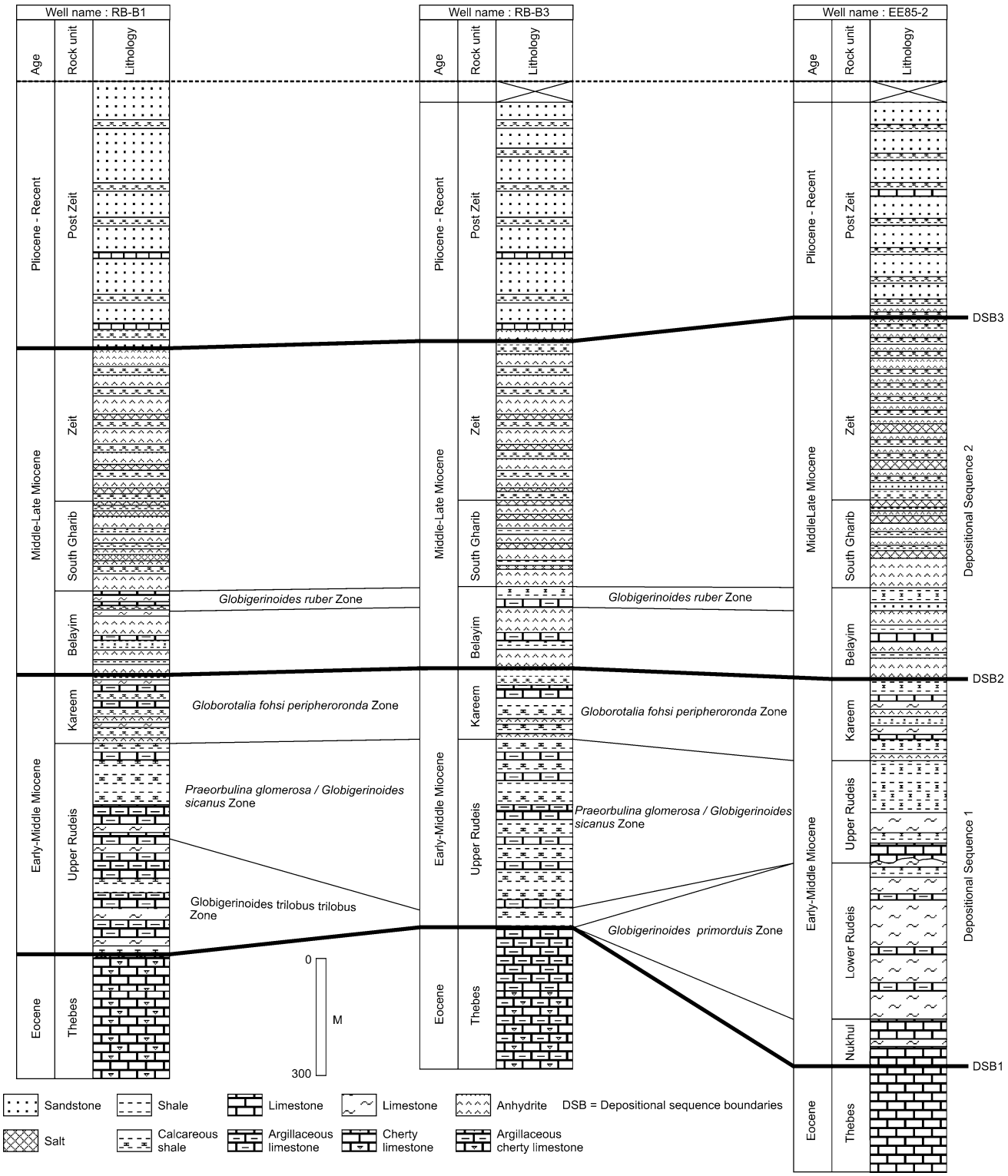

Fig. 5 Biostratigraphic correlation between the three studied wells RB-B1, RB-B3 and EE85-2. This figure shows also the correlated two depositional sequences and their bounding sequence boundaries (DSB1, DSB2 and DSB3) between these wells

(Hewaidy et al. 2013, Fig. 7). The Kareem Formation is subdivided into Markha and Shagar members (Bosworth and McClay 2001, Figs. 3, 4). The appearance of the first Middle Miocene evaporites of the lower Markha Member (Figs. 3, 4) denotes the abrupt facies change and basin restriction during the deposition of early Kareem

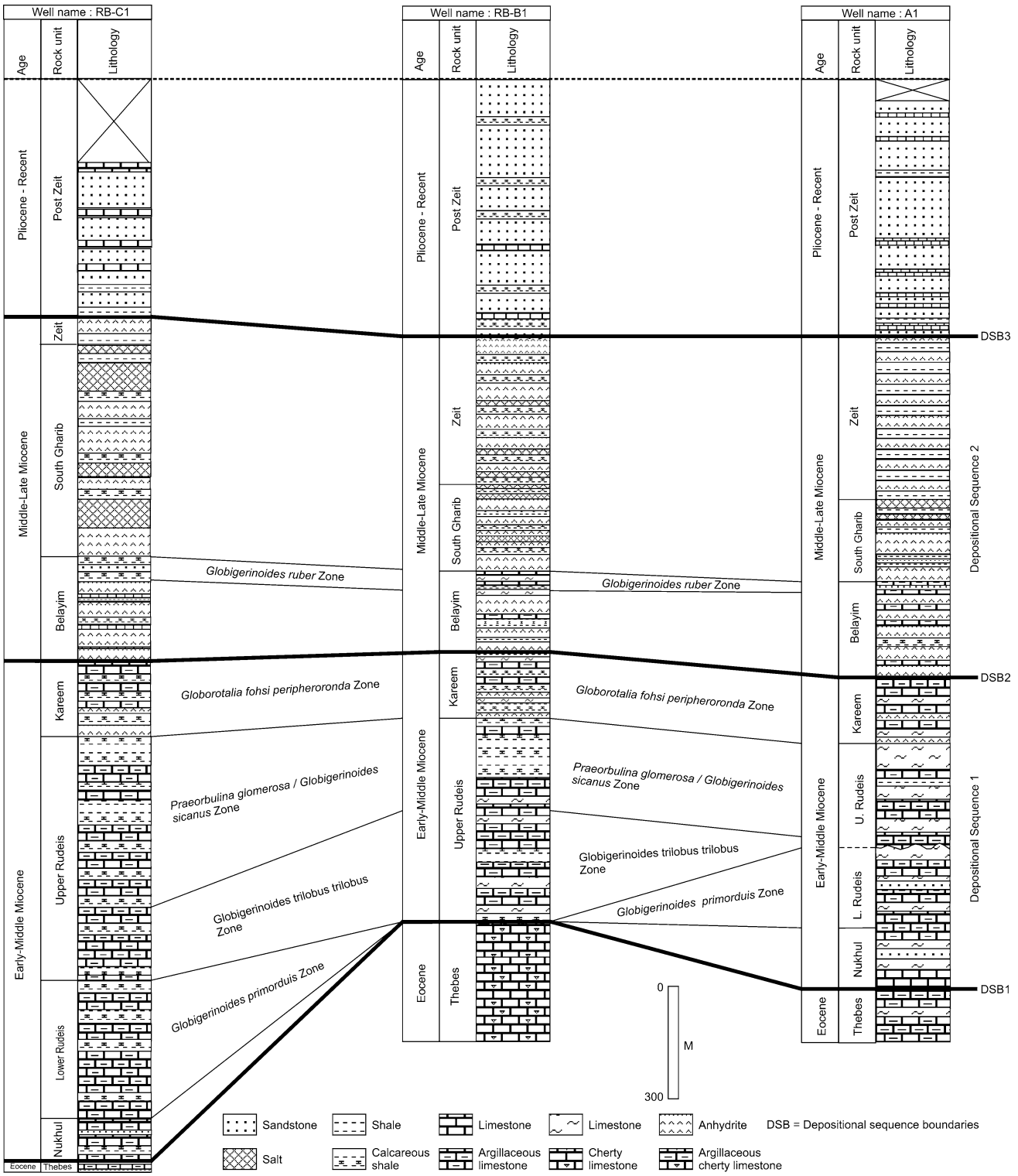

Fig. 6 Biostratigraphic correlation between the three studied wells RB-C1, RB-B1 and RB-A1. This figure reveals also the correlated two depositional sequences and their bounding sequence boundaries (DSB1, DSB2 and DSB3) between these wells

Formation time (Bosworth and McClay 2001). The boundary between the Rudeis and Kareem formations is marked by differential uplift due to renewed block rotation; in the southern Gulf region contemporaneous with the continuation of the "mid-clysmic" or "mid-Rudeis" event (Patton et al. 1994; Bosworth and McClay 2001).

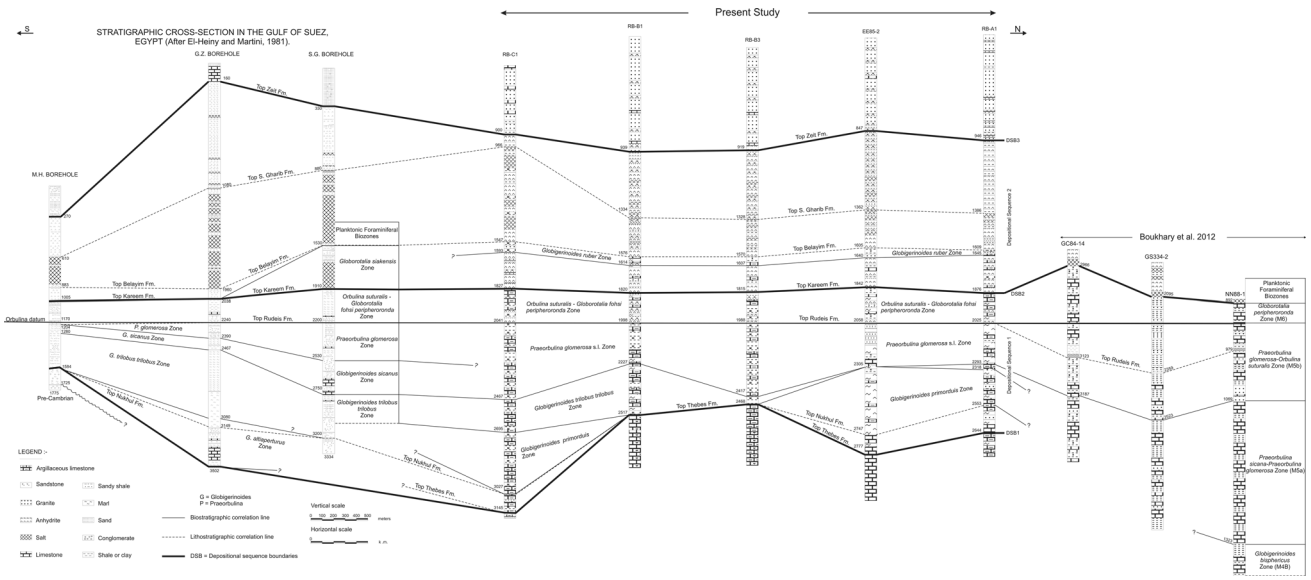

Fig. 7 Correlation between the five studied wells with those established by El-Heiny and Martini (1981) and Boukhary et al. (2012). The correlated two depositional sequences and their bounding sequence boundaries (DSB1, DSB2 and DSB3) between the studied wells are also extended along wells of El-Heiny and Martini (1981) from the southwestern flank of the Gulf of Suez (Fig. 1)

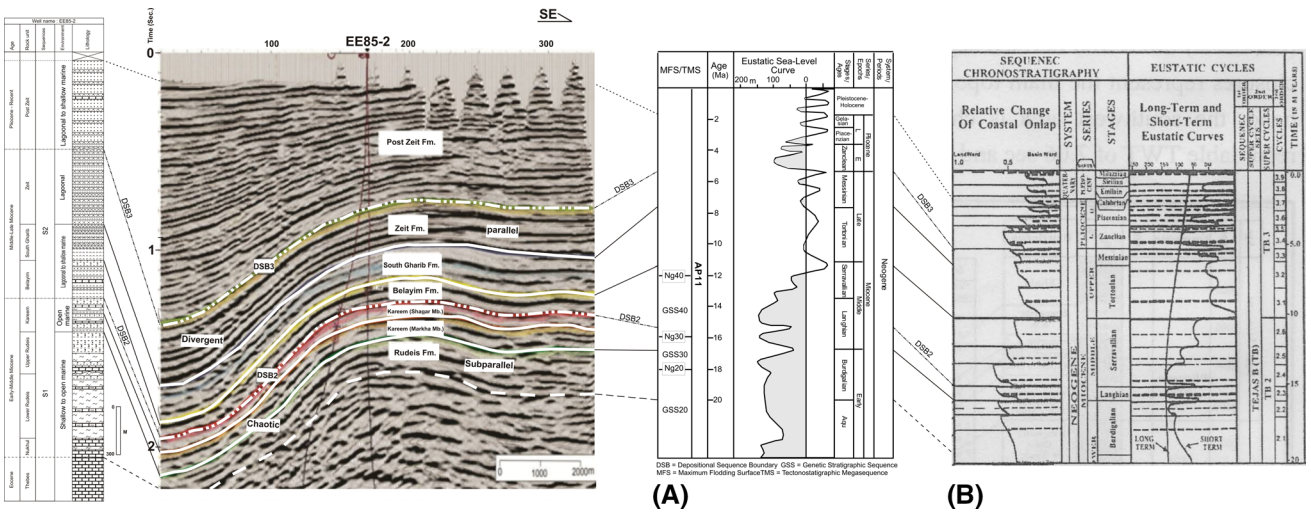

Fig. 8 Lithologic section of the Miocene succession well EE85-2 (*left*) correlated with the interpreted major depositional sequence boundaries of the seismic section Crossline 315 (*middle*) and **a** the Arabic Platform Cycle Chart (modified after Sharland et al. 2001; Haq and Al-Qahtani 2005), **b** the global sea level curve of Haq et al. (1987)

3.4 The Belayim Formation

The Middle Miocene (Late-Serravallian, Evans 1990) Belayim Formation consists mainly of anhydrites, argillaceous limestones and Calcareous shales (Figs. 3, 4, 5, 6, 7). This formation unconformably overlies the Kareem Formation (Bosworth and McClay 2001) and its thickness varies from 237 m in well EE85-2 to 280 m in well RB-C1 (Fig. 7). The deposition of the evaporites of this formation denotes a major vertical facies change in the Gulf of Suez rift basin (Bosworth and McClay 2001). The base of this formation coincides with the upper depositional sequence boundary (DSB2) of the lower depositional sequence (Figs. 2, 3, 4, 5, 6, 7, 8, 9, 10, 11, see Sect. 5 for more discussion).

3.5 The South Gharib Formation

South Gharib Formation consists mainly of salts, anhydrites and calcareous shales with few limestones interbeds (Figs. 3, 4, 5, 6, 7). This formation conformably overlies the Belayim Formation and its thickness varies from 223 m in well RB-A1 to 581 m in well RB-C1 (Fig. 7).

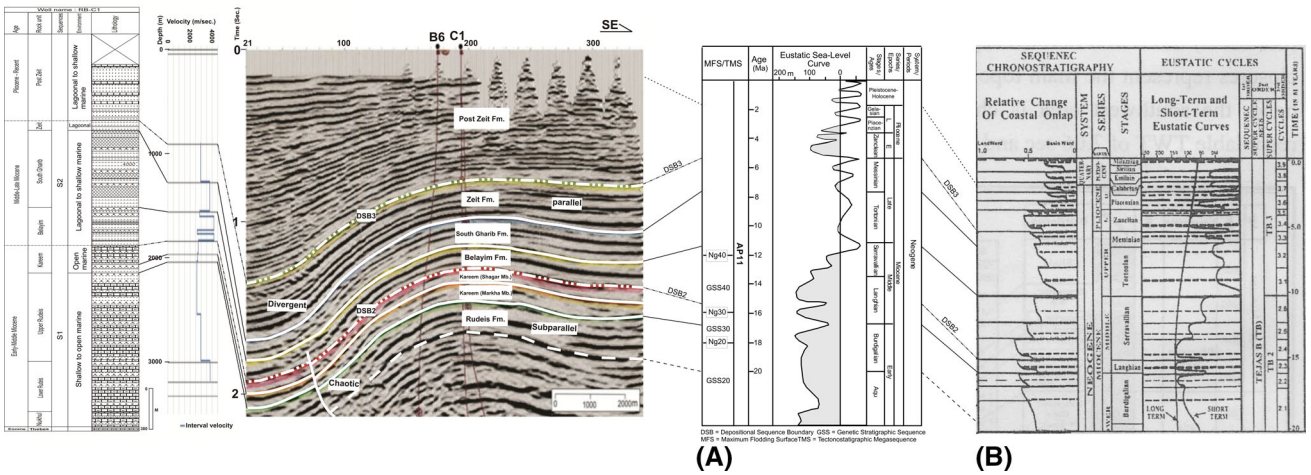

Fig. 9 Lithologic section of the Miocene succession well RB-C1 and its interval velocity (m/s) (*left*) correlated with the interpreted major depositional sequence boundaries of the seismic section Crossline 255 (*middle*) and **a** the Arabic Platform Cycle Chart (modified after Sharland et al. 2001; Haq and Al-Qahtani 2005), **b** the global sea level curve of Haq et al. (1987)

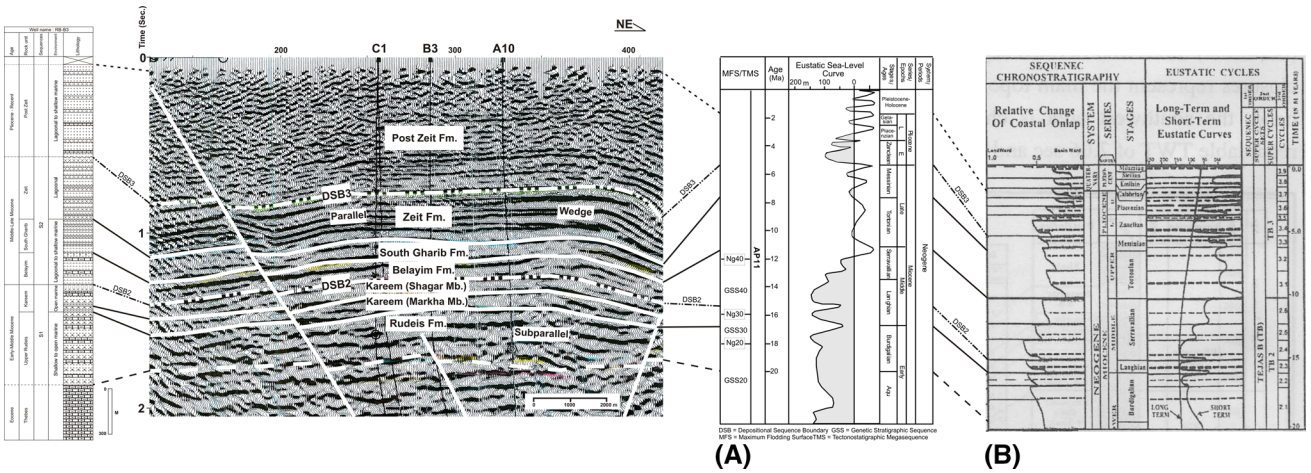

Fig. 10 Lithologic section of the Miocene succession well RB-B3 (*left*) correlated with the interpreted major depositional sequence boundaries of the seismic section Inline 200 (*middle*) and **a** the Arabic Platform Cycle Chart (modified after Sharland et al. 2001; Haq and Al-Qahtani 2005), **b** the global sea level curve of Haq et al. (1987)

3.6 The Zeit Formation

Zeit Formation consists mainly of anhydrites and calcareous shales besides salts at the southeast (Figs. 3, 4). This formation conformably overlies the South Gharib Formation with thickness variations from 66 m in well RB-C1 to 515 m in well EE85-2 (Fig. 7). The Late Miocene (Messinian) Zeit Formation is unconformably underlain the Pliocene post-Zeit Formation (Figs. 2, 3, 4, 5, 6, 7, 8, 9, 10, 11). This unconformity surface, which separates these two formations marks the top anhydrite bed of the Zeit Formation (Evans 1988). The top of this formation coincides with sequence boundary DSB3 of the upper depositional sequence (Figs. 2, 3, 4, 5, 6, 7, 8, 9, 10, 11, see Sect. 5 for more discussion).

3.7 The post-Zeit formation

The facies of the post-Zeit formation varies from mainly anhydrites and sandstones, limestones and calcareous shales to sandstones and limestones at the southwest (Figs. 3, 4). The thickness of this varies from 900 m in well RB-C1 to 946 m in well RB-A1 (Fig. 7).

4 Biostratigraphy

This part deals with the biostratigraphy of the Miocene sequence in the northern part of the Gulf of Suez, Egypt. According to the available data, the described index taxa and the identified biozones are based mainly on the

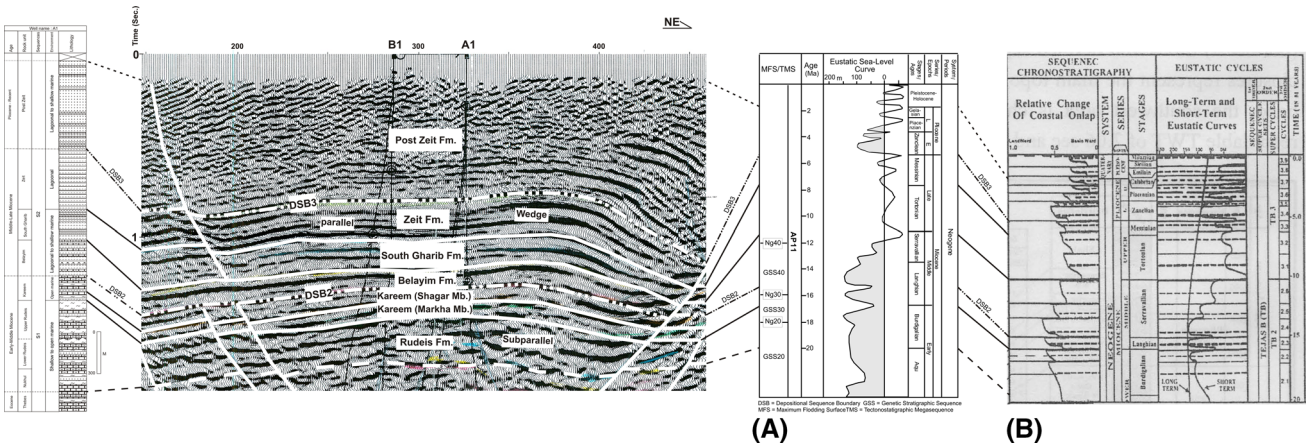

Fig. 11 Lithologic section of the Miocene succession well RB-A1 (*left*) correlated with the interpreted major depositional sequence boundaries of the seismic section Inline 170 (*middle*) and **a** the Arabic Platform Cycle Chart (modified after Sharland et al. 2001; Haq and Al-Qahtani 2005), **b** the global sea level curve of Haq et al. (1987)

palaeontologic data taken from composite logs of the Suez Oil Company (SUCO) (Figs. 5, 6, 7). The herein applied zonal scheme is based primarily on a planktonic foraminiferal biozonal scheme of Bolli and Saunders (1985).

4.1 Planktonic foraminiferal biozones

The five planktonic foraminiferal biozones (Figs. 5, 6, 7) recognised in the studied five boreholes (RB-A1, RB-B1, RB-B3, EE85-2 and RB-C1, location indicated in Fig. 1) are compared well to those of El-Heiny and Martini (1981) and Boukhary et al. (2012) (Fig. 7) and are briefly discussed from base to top as follows:

4.1.1 Globigerinoides primordius Zone

Category: Concurrent range zone

Age: Early Miocene (Aquitanian)

Author: Blow (1969)

Definition: Interval from first occurrence of frequent *Globigerinoides primordius/trilobus* s.l. to last occurrence of *Globorotalia kugleri* Zone.

Remarks: This zone is recorded from wells RB-A1, EE85-2 and East RB-C1 (Figs. 5, 6, 7) while it is missing in wells RB-B1 and RB-B3. The thickness of this biozones ranges from 235 m in well RB-A1 to 442 m in well EE85-2 and it spans the Lower Rudeis Member (Figs. 5, 6, 7). The absence of this zone in wells RB-B1 and RB-B3 is related to the "mid-clysmic" or "mid-Rudeis" event following the deposition of the Lower Rudeis Member resulted in uplift and erosion of this member (Figs. 5, 6). The *Globigerinoides trilobus trilobus* Zone in wells RB-A1, EE85-2 and East RB-C1 (Figs. 5, 6, 7) unconformably overlie this zone. The absence of *G. primordius* Zone in El-Heiny and Martini (1981) may also be related to the "mid-clysmic" or "mid-Rudeis" event (Figs. 5,6, 7). *G. primordius* Zone is equivalent to the *Globoquadrina binaiensis* (M2) partial-range Zone of Berggren et al. (1995) and Wade et al. (2011) and *G. primordius* Zone of Hewaidy et al. (2016). In Egypt, this zone is recorded from the base of the Rudeis Formation (Andrawis and Abdel Malik 1981; El-Heiny and Martini 1981; Haggag et al. 1990; Mandur 2009; Hewaidy et al. 2012, 2016).

4.1.2 Globigerinoides trilobus trilobus Zone

Category: Interval zone

Age: Burdigalian, Early Miocene

Author: Bizon and Bizon (1972)

Definition: Interval from last occurrence of *G. altiaperturus* to first occurrence of *Praeorbulina glomerosa*.

Remarks: This zone is recorded from RB-A1, RB-B1, RB-B3 and RB-C1 (Figs. 5, 6, 7) while it is missing in well EE85-2. The thickness of this biozone ranges from 25 m in well RB-A1 to 290 m in well RB-B1and it spans the lower part of the Upper Rudeis Member (Figs. 5, 6, 7). The *P. glomerosa* s.l. Zone overlies this zone (Figs. 5, 6, 7). *Globigerinoides trilobus trilobus* Zone is correlated well to that of El-Heiny and Martini (1981) (Fig. 7). *Globigerinoides trilobus trilobus* Zone is equivalent to the *G. trilobus* Zone which was recorded by many authors (Haggag et al. 1990; Phillip et al. 1997; Hewaidy et al. 2016) and to the *C. dissimilis/Praeorbulina sicana* (M4) Zone of Hewaidy et al. (2013).

4.1.3 Praeorbulina glomerosa s.l. Zone

Category: Lineage zone

Age: Langhian, Early Miocene

Author: Bizon and Bizon (1972)

Definition: Interval from first occurrence of *P. glomerosa* to first occurrence of *Orbulina suturalis*.

Remarks: This zone is found in wells RB-A1, RB-B1, RB-B3, EE85-2 and RB-C1 (Figs. 5, 6, 7). The thickness of this zone ranges from 229 m in well RB-B1 to 429 m in well RB-B3 and it spans the upper part of the Upper Rudeis Member (Figs. 5, 6, 7). It is conformably overlain by the *Globorotalia fohsi peripheroronda* Zone (Fig. 5, 6, 7). *P. glomerosa* s.l. Zone is equivalent to that of El-Heiny and Martini (1981) (Fig. 7). *P. glomerosa* s.l. Zone could be correlated to the *P. glomerosa* Zone of Kerdany (1968) in the Gulf of Suez, and Farouk et al. (2014) in the Nile Delta. It is equivalent to the *P. glomerosa* Zone described by Bolli (1957, 1966), Stainforth et al. (1975), and Postuma (1971). This zone is equated to the lower part of the *P. sicanus*/*O. suturalis* Zone (M5) of Hewaidy et al. (2013) and *P. glomerosa*/*O. suturalis* Zone (M5b) of Boukhary et al. (2012) (Fig. 7).

4.1.4 Orbulina suturalis: Globorotalia fohsi peripheroronda Zone

Category: Concurrent range zone

Age: Langhian-Serravallian, Early to Middle Miocene

Author: Bizon and Bizon (1972)

Definition: Interval from first occurrence of *O. suturalis* to last occurrence of *Globorotalia fohsi peripheroronda*.

Remarks: This zone is recorded in wells RB-A1, RB-B1, RB-B3, EE85-2 and RB-C1 (Figs. 5, 6, 7). The thickness of this biozone ranges from 149 m in well RB-A1 to 216 m in well EE85-2 and it spans the Kareem Formation (Figs. 5, 6, 7). This biozone is unconformably overlain by the depositional sequence boundary DSB2 (Figs. 5, 6, 7). *O. suturalis*—*Globorotalia fohsi peripheroronda* Zone is correlated well to that of El-Heiny and Martini (1981) (Fig. 7). *O. suturalis*—*Globorotalia fohsi peripheroronda* Zone could be correlated with *G. peripheroronda* (M6) Zone of Hewaidy et al. (2013) and Boukhary et al. (2012) (Fig. 7).

4.1.5 Globigerinoides ruber zone

Category: Interval zone

Age: Middle Miocene

Author: Bolli (1966)

Definition: Interval with zonal marker from last occurrence of *Globorotalia fohsi robusta* to last Miocene occurrence of zonal marker.

Remarks: This zone is found in wells RB-A1, RB-B1, RB-B3, EE85-2 and RB-C1 (Figs. 5, 6, 7). The thickness of this biozone ranges from 36 m in well RB-A1 to 46 m in well RB-C1 and it spans the upper part of the Belayim Formation (Figs. 5, 6, 7). The lower part of this formation is barren (see also Hewaidy et al. 2016). This biozone is not recorded in El-Heiny and Martini (1981) (Fig. 7).

5 Sequence stratigraphy and seismic facies analysis

Seismic facies analysis of the Miocene succession allows to divide the seismic sections into depositional sequences bounded by sequence boundaries according to Vail et al. (1977a, b, c), (Vail 1987), Wagoner et al. (1988, 1990), Posamentier and Weimer (1993), Emery and Myers (1996), Catuneanu (2006). Some interpreted seismic sections are tied with the composite lithologic logs of the wells to detect the exact sequence boundaries and the possible causes of seismic amplitude variations.

The studied Miocene succession in the northern part of the Gulf of Suez is subdivided into two major third order depositional sequences (S1 and S2) separated by the three major depositional sequence boundaries (DSB1, DSB2 and DSB3, Figs. 2, 3, 4, 5, 6, 7, 8, 9, 10, 11). The latter correspond well with the major unconformity surfaces along the palaeobathymetry of Naggar and El-Hilaly (1985) (Fig. 2). The environment of deposition and tectonic activities during the deposition of these two major depositional sequences are described by Naggar and El-Hilaly (1985) (Fig. 2). These sequences illustrated on five studied wells, are traced on the southwestern flank of the Gulf of Suez by correlating them with El-Heiny and Martini (1981) (Fig. 7). They well correlate with the genetic stratigraphic sequences (GSS20, GSS30 and GSS40), separated by the maximum flooding surfaces MFS N20 and MFS Ng30 respectively, of the major tectonostratigraphic megasequence (AP11) of the Arabian Plate, according to Sharland et al. (2001); Haq and Al-Qahtani (2005) (Figs. 8, 9, 10, 11). These sequences also correlated with the global sea level curve of Haq et al. (1987) (Figs. 8, 9, 10, 11).

5.1 The first depositional sequence (S1)

This sequence includes the Lower-Middle Miocene rocks of Nukhul, Rudeis and Kareem Formations (Figs. 2, 3, 4, 5, 6, 7, 8, 9, 10, 11). The base of this sequence is bounded by the depositional sequence boundary (DSB1, Figs. 2, 5, 6, 7). This boundary is marked by regression, uplift, erosion of the uplifted part that is also affected by a following volcanic activity as a result of rifting during Oligocene and local deposition of Abu Zenima red beds in the localised

starved basins (Fig. 2). S1 sequence boundary may be equivalent to SB3 sequence boundary of (Hewaidy et al. 2013). The latter may coincided with a world short-term sea level fall (Miller et al. 2005) and it is referred as a true erosional surface typifying a significant gulf-wide depositional hiatus (Patton et al. 1994; Sharp et al. 2000; El-Azabi 2004).

On the other hand, this boundary cannot be followed on the seismic sections, because they are poorly processed (Figs. 3, 4, 8, 9, 10, 11). The seismic facies of this sequence (Figs. 8, 9, 10, 11) is characterised by sheet-like external forms, concordant reflection geometry along the upper boundary of the sequence, regular configuration modifier, chaotic to subparallel principal internal configurations, moderate amplitudes and discontinuous horizons. The Nukhul Formation is composed of mainly limestones and sandstones filling up the topography lows during earliest Miocene. These lows were created during Oligocene differential uplift (Patton et al. 1994). The thickness of this formation is small along the study area, while, it is absent at the middle part due to uplift and erosion associated with tilting and rotation of the fault blocks coupled with the onset of rifting in the Gulf of Suez (Naggar and El-Hilaly 1985; Patton et al. 1994; Bosworth and McClay 2001, Fig. 7).

The Rudeis Formation is subdivided into Lower Rudeis and Upper Rudeis members (Bosworth and McClay 2001). The boundary between these two rock units marks the "mid-Rudeis" or "mid-Clysmic" event as unconformity surface (Chowdhary and Taha 1987; Naggar and El-Hilaly 1985; Patton et al. 1994). This boundary may be equated to SB4 sequence boundary of Hewaidy et al. (2013). SB4 sequence boundary may be coincided with a world short-term sea level fall (Miller et al. 2005) and it is described as an important disconformity between the Lower Rudeis and Upper Rudeis rock units (El-Azabi 2004). The Lower Rudeis Member is composed mainly of limestones and calcareous sandstones with few shales deposits relatively rich in both planktic and benthic foraminifera, indicating deposition in a deeper marine environment. This indicates an Early Miocene transgression (Naggar and El-Hilaly 1985, Fig. 2).

The Upper Rudeis Member consists mainly of limestones, argillaceous limestones, calcareous shales, marl and sandstone, which is even richer in microfossils, deposited in a relatively deep marine environment. This indicates continued rising in sea level or transgression (Naggar and El-Hilaly 1985, Fig. 2). The sliding and detachment of the blocks close to the rift margin results in sites available for sediments accumulation, reflecting a rapid rate of sedimentation and hence the formation of lenticular bodies (Lashin and Abd El-Aal 2004). The Kareem Formation is composed mainly of calcareous shales, marl, argillaceous limestones with two to three thick layers of massive anhydrites. The Kareem Formation lithologically reflects marine transgression and sedimentation in deep marine environment, with minor episodes of basin closing and restricted circulation, which account for the deposition of evaporates.

The top of the third order sequence is bounded by the depositional sequence boundary (DSB2, Figs. 2, 3, 4, 5, 6, 7, 8, 9, 10, 11). This boundary is defined as unconformity surface between the Kareem Formation and its overlying Belayim Formation according to Bosworth and McClay (2001). DSB2 sequence boundary may be equivalent to SB7 sequence boundary of Hewaidy et al. (2013), which resulted from the effect of the post-Kareem tectonic event (Evans 1988). SB7 sequence boundary was also recorded by El-Azabi (2004) in west-central Sinai, by Hewaidy et al. (2013) in the eastern side of the Gulf of Suez. This sequence boundary referred as marked basin-wide unconformity above the pre-rift sequence boundary in the northern Gulf of Suez (Dolson et al. 1996) and it is contemporaneous with a world short-term sea level fall, which took place at the Langhian/Serravallin boundary (Miller et al. 2005).

The S1 third order depositional sequence comprises four planktonic foraminiferal biozones (*G. primordius*, *Globigerinoides trilobus trilobus*, *P. glomerosa* s.l. and *O. suturalis—Globorotalia fohsi peripheroronda*) of Early-Middle Miocene age (Figs. 5, 6, 7). This sequence is correlated well with the two genetic stratigraphic sequences GSS20 and GSS30 of the major tectonostratigraphic Megasequence AP11 of the Arabian Plate (Sharland et al. 2001; Haq and Al-Qahtani 2005, Figs. 8, 9, 10, 11). These two genetic sequences resulted from subsidence enhanced by eustacy (Sharland et al. 2001, Figs. 8, 9, 10, 11). This subsidence may be contemporaneous with the rapid subsidence of "mid-Clysmic" event during the deposition of the upper Rudeis Member, which continued during the deposition of the Kareem Formation.

5.2 The second depositional sequence (S2)

This sequence comprises the Middle-Upper Miocene rocks of Belayim, South Gharib and Zeit Formations (Figs. 2, 3, 4, 5, 6, 7, 8, 9, 10, 11). The depositional environment of this sequence is considered to be lagoonal to shallow marine environment. The base of this sequence is bounded by the depositional sequence boundary (DSB2), while this sequence is topped by the depositional sequence boundary (DSB3, Figs. 2, 3, 4, 5, 6, 7, 8, 9, 10, 11). DSB3 between Zeit and post-Zeit formations (Figs. 8, 9, 10, 11) is referred as marked basin-wide unconformity in the Gulf of Suez (Patton et al. 1994; Bosworth and McClay 2001) and it is contemporaneous with a world short-term sea level fall.

The seismic facies of this sequence (Figs. 8, 9, 10, 11) is characterised by wedge-shaped and even sheet-like external forms, concordant along the upper boundary of the sequence, concordant reflection geometries are recorded along the lower boundary, regular configuration modifier, divergent to parallel principal internal configurations, low to high amplitudes and continuous horizons. The Belayim, South Gharib and Zeit Formations were deposited essentially in a basin with restricted marine circulation. The alteration of clastics with evaporite levels points to periodic influx of clastics from high shoulders. This scenario is reduced with time and became negligible during the deposition of the South Gharib and Zeit formations (Naggar and El-Hilaly 1985).

This third order sequence is correlated well with the genetic stratigraphic sequence GSS40 of the major tectonostratigraphic Megasequence AP11 of the Arabian Plate (Sharland et al. 2001; Haq and Al-Qahtani 2005, Figs. 8, 9, 10, 11). This late Serravallian third order GSS40 is also driven by subsidence enhanced by eustacy (Sharland et al. 2001, Figs. 8, 9, 10, 11). The post-Miocene is composed mainly of sandstones with few siltstones and thin-bedded limestones and anhydrites, and the tectonic-environment of deposition is uplift followed by deposition under lagoonal to shallow marine environment (Naggar and El-Hilaly 1985, Fig. 2). The lithologic composition of the post-Miocene rocks may indicate a near detrital source filling topograhic depressions. That may have been inundated occasionally with sea water in times of short-time high stands or subsidence and hence, the deposition of evaporitic and laminated shallow limestone layers.

6 Conclusions

Seismic stratigraphic study helped in recognizing sequence boundaries and shed light on the syn-rift history of the northern Gulf of Suez during the Miocene. The present work deals with the study of northern part of the Gulf of Suez, in terms of interpreting the sequence stratigraphy, biostratigraphy and depositional environments through evaluating the seismic stratigraphic and seismic-facies analysis of the area. Seismic interpretations are carried out on 34 3D seismic profiles passing through the study area. The lithofacies of the syn-rift formations was described based on the lithology of these formations encountered in ten wells and geologic interpretation of two seismic profiles distributed along the offshore northern part of the Gulf of Suez region.

The biostratigraphy of the Miocene sequence in this study resulted in the recognition of five planktonic foraminiferal biozones in the boreholes (RB-A1, RB-B1, RB-B3, EE85-2 and RB-C1). Sequence stratigraphy and seismic facies analysis of the Miocene succession were carried out to delineate sequence boundaries. The Miocene succession in the northern part of the Gulf of Suez is subdivided into two major third order depositional sequences (S1 and S2) separated by the three major depositional sequence boundaries (DSB1, DSB2 and DSB3). They are traced to the southwestern flank of the Gulf of Suez by correlating them with El-Heiny and Martini (1981). They are also correlated well with the global sea level curve of Haq et al. (1987) and the genetic stratigraphic sequences (GSS20, GSS30 and GSS40), separated by the maximum flooding surfaces MFS N20 and MFS Ng30 respectively, of the major tectonostratigraphic megasequence (AP11) of the Arabian Plate, according to Sharland et al. (2001); Haq and Al-Qahtani (2005).

Acknowledgements The authors wish to thank Prof. Omar Cherif, Egyptian National Authority, for Remote Sensing and Space Sciences (NARSS), Egypt, and D. Radwan Abdulnasr, Geology Department, Faculty of Education, Ain Shams University, for reviewing the manuscript.

References

Andrawis, S. F., & Abdel Malik, W. M. (1981). Lower/middle Miocene boundary in the Gulf of Suez region, Egypt. *Newsletters on Stratigraphy, 10,* 156–163.

Berggren, W. A., Swisher, C. C., & Aubry, M. P. (1995). A revised Cenozoic geochronology and chronostratigraphy. In: Geochronology time scales and global stratigraphic correlation. *Society of Sedimentary Geology, 54,* 277–302.

Bizon, G., & Bizon, J. J. (1972). *Atlas des principaux foraminiferes planctoniques du basin méditerranéen. Oligocéne á Quaternaire*. Paris: Editions Technip.

Blow, W. H. (1969). Late middle eocene to recent planktonic foraminiferal biostratigraphy. In P. Bronnimann, & H. H Renz (Eds), *Proceedings of the first international conference on planktonic microfossils* (Geneva, 1967), vol. 1 (pp. 199–421). Leiden, E. H., Brill.

Bolli, H. M. (1957). Planktonic foraminifera from the Oligocene-Miocene Cipero and Lengua formations of Trinidad, B.W.I. In A. R. Loeblich, H. Tappan, J. P. Beckmann, H. M. Bolli, E. M. Gallitelli, & J. C. Troelsen (Eds.), *Studies in Foraminifery, Bulletin of the U.S. National Museum* (pp. 97–123). Vol. 215.

Bolli, H. M. (1966). Zonation of Cretaceous to Pliocene marine sediments based on planktonic foraminifera. *Boletin Informativo Asociaciòn Venezolana de Geologà, Minerarà Petro, 9,* 3–32.

Bolli, H. M., & Saunders, J. B. (1985). Oligocene to Holocene low latitude planktonic foraminifera. In H. M. Bolli, J. B. Saunders, & K. Perch-Nielsen (Eds.), *Plankton stratigraphy* (pp. 155–262). Cambridge: Cambridge University Press.

Bosworth, W. (1995). A high-strain rift model for the southern Gulf of Suez. Egypt. In J. J. Lambiase (Ed.), *Hydrocarbon habitat in rift basins*, Vol. 80 (pp. 75–112). Geological Society, London: Special Publications.

Bosworth, W., & McClay, K. (2001). Structural and stratigraphic evolution of the Gulf of Suez rift, Egypt: A synthesis. In P. A. Ziegler, W. Cavazza, A. H. F. Robertson, & S. Crasquin-Soleau (Eds.), *Peri-Tethys Memoir 6: Peri-Tethyan rift/wrench basins and passive margins* (pp. 567–606). Vol. 186, Paris: Museum National d'Histoire naturelle de Paris, Memoirs.

Boukhary, M., Abd El Naby, A. I., Faris, M., & Morsi, A. M. (2012). Plankton stratigraphy of the early and middle Miocene Kareem and Rudeis formations in the central part of the Gulf of Suez, Egypt. *Historical Biology, 24*(1), 49–62.

Catuneanu, O. (2006). *Principles of sequence stratigraphy* (p. 8). Amsterdam: Elsevier.

Chowdhary, L. R., & Taha, S. (1987). Geology and habitat of oil in Ras Budran field, Gulf of Suez, Egypt. *American Association of Petroleum Geologists, 71*(10), 1274–1293.

Colletta, B., Le Quellec, P., Letouzy, J., & Moretti, I. (1988). Longitudinal evolution of the Suez rift structure, Egypt. *Tectonophysics, 153,* 221–233.

Dolson, J., El Gendi, O., Charmy, H., Fathalla, M., & Gaafr, I. (1996). Gulf of Suez rift basin sequence models—Part A., Miocene sequence stratigraphy and exploration significance in the greater October field area, northern Gulf of Suez. *13th E.G.P.C. Exploration and Production Conference* (pp 227–241). Cairo, Egypt.

El-Azabi, M. H. (2004). Facies characteristics, depositional styles and evolution of the Syn-rift Miocene sequences in Nukhul-Feiran area, Sinai side of the Gulf of Suez rift basin, Egypt. *Sedimentology, Egypt, 12,* 69–103.

El-Heiny, I., & Martini, E. (1981). Miocene foraminifera and calcareous nannoplankton assemblages from the Gulf of Suez region and correlations. *Geology of the Mediterranean, 8*(2), 101–108.

Emery, D., & Myers, K. (1996). *Sequence stratigraphy*. Oxford: Blackwell Science. Ltd.

Evans, A. L. (1988). Neogene tectonic and stratigraphic events in the Gulf of Suez rift area, Egypt. *Tectonophysics, 153,* 235–247.

Evans, A. L. (1990). Miocene sandstone provenance relationships in the Gulf of Suez: Insights into syn-rift unroofing and uplift history. *American Association of Petroleum Geologists, 74,* 1386–1400.

Farouk, S., Ziko, A., Eweda, S., & Said, A. E. (2014). Subsurface Miocene sequence stratigraphic framework in the Nile Delta, Egypt. *Journal of African Earth Sciences, 91,* 89–109.

Garfunkel, R. L., & Bartov, Y. (1977). The tectonic of the Suez rift. *Geological Survey of Israel, Bulletin, 71,* 1–44.

Haggag, M. A., Youssef, I., & Salama, G. R. (1990). Stratigraphic and phylogenetic relationships of Miocene planktonic foraminifera from the Gulf of Suez, Egypt. M.E.R.C, Ain Shams University. *Earth Sci, 4,* 22–40.

Haq, B. U., & Al-Qahtani, A. M. (2005). Phanerozoic cycles of sea-level change on the Arabian platform. *Geo Arabia, 10*(2), 127–160.

Haq, B. U., Hardenbol, J., & Vail, P. R. (1987). Chronology of fluctuating sea level since the Triassic. *Science, 235,* 1156–1167.

Hewaidy, A. A., Farouk, S., & Ayyad, H. M. (2012). Nukhul formation in Wadi Baba, southwest Sinai Peninsula, Egypt. *Geoa, 17,* 103–120.

Hewaidy, A. A., Farouk, S., & Ayyad, H. M. (2013). Foraminifera and sequence stratigraphy of Burdigalian–Serravallian succession on the eastern side of the Gulf of Suez, southwestern Sinai, Egypt. *Neues Jb Geol Paläontol Abh, 2,* 151–170.

Hewaidy, A. A., Mandur, M. M., Farouk, S., & El Agroudy, I. S. (2016). Integrated planktonic stratigraphy and palaeoenvironments of the Lower-Middle Miocene successions in the central and southern parts of the Gulf of Suez, Egypt. *Arabian Journal of Geosciences, 9,* 159.

Kerdany, M. T. (1968). Note on the planktonic zonation of the Miocene in the Gulf of Suez Region U.A.R. *Proceedings of the Committee of Mediterranean Neogene Stratigraphy, 35,* 157–166.

Lashin, A., & Abd El-Aal, M. (2004). Seismic data analysis to detect the depositional process environments and structural framework of the east central part of Gharib Province, Gulf of Suez-Egypt. *Annals of the Egyptian Geological Survey, 27,* 523–550.

Mandur, M. M. (2009). Calcareous nannoplankton biostratigraphy of the lower and middle Miocene of the Gulf of Suez, Egypt. *Aust J Basic Appl Sci, 3*(3), 2290–2303.

McClay, K. R., Nichols, G. J., Khalil, S., Darwish, M., & Bosworth, W. (1998). Extensional tectonics and sedimentation, eastern Gulf of Suez, Egypt. In B. H. Purser & D. V. V. J. Bosence (Eds.), *Sedimentation and tectonics of rift basins, Red Sea-Gulf of Aden* (pp. 223–238). London: Chapman and Hall.

Miller, K. G., Kominz, M. A., Browning, J. V., Wright, J. D., Mountain, G. S., Katz, M. E., et al. (2005). The Phanerozoic record of global sea-level change. *Science, 310,* 1293–1298.

Moustafa, A. R. (1993). Structural characteristics and tectonic evolution of the east margin blocks of the Suez rift. *Tectonophysics, 223,* 381–399.

Naggar, A. A., & El-Hilaly, H. (1985). Geological aspects and reservoir units of Ras Budran field; Egyptian General Petroleum Corporation. *8th production seminar* (pp. 1–12). Egypt.

Omar, G. I., Steckler, M. S., Buck, W. R., & Kohn, B. P. (1989). Fission-track analysis of basement apatites at the western margin of the Gulf of Suez rift, Egypt: evidence for synchroneity of uplift and subsidence. *Earth and Planetary Science Letters, 94,* 316–328.

Ouda, K. H., & Masoud, M. (1993). Sedimentation history and geological evaluation of the Gulf of Suez during the late Oligocene-Miocene. *Geological Society of Egypt, Special Publications, 1,* 47–88.

Patton, T. L., Moustafa, A. R., Nelson, R. A., & Abdine, S. A. (1994). Tectonic evolution and structural setting of the Suez Rift. In: S. M. London (Ed.), *Interior rift basins; American Association of Petroleum Geologists* (pp. 7–55). Memoirs, 59.

Phillip, G., Imam, M. M., & Abdel Gawad, G. I. (1997). Planktonic foraminiferal biostratigraphy of the Miocene sequence in the area between Wadi El-Tayiba and Wadi Sidri, west central Sinai, Egypt. *J Afr Earth Sci., 25*(3), 435–451.

Posamentier, H. W., & Weimer, P. (1993). Siliciclastic sequence stratigraphy and petroleum geology-where to from here? *AAPG Bulletin, 77,* 731–742.

Postuma, J. A. (1971). *Manual of planktonic foraminifera*. Amsterdam: Elsevier Publishing.

Richardson, M., & Arthur, M. A. (1988). The Gulf of Suez-northern Red Sea neogene rift: A quantitive basin analysis. *Marine Arid Petroleum Geology, 5,* 247–270.

Schlumberger (1984). *Well evaluation conference* (p 60). Egypt.

Schlumberger Limited (1995). *Algeria well evaluation conference* (p 87). Egypt; Houston, Texas, USA.

Scott, R. W., & Govean, F. M. (1985). Early depositional history of a rift basin: Miocene in the western Sinai. *Palaeogeography, Palaeoclimatology, Palaeoecology, 52,* 143–158.

Sharland, P. R., Archer, R., Casey, D. M., Davies, R. B., Hall, S. H., Heward, A. P., Horbury, A. D., & Simmons, M. D. (2001). *Arabian plate sequence stratigraphy*. Geoarabia, Gulf PetroUnk, Bahrain, Spec. Publ. 2.

Sharp, I. R., Gawthorp, R. L., Armstrong, B., & Undcrhill, J. R. (2000). Propagation history and passive rotation of mesoscale normal faults: implication for syn-rift stratigraphic development. *Basin Research, 12,* 285–306.

Stainforth, R. M., Lamb, J. L., Luterbacher, H., Beard, J. H., & Jeffords, R. M. (1975). Cenozoic planktonic foraminiferal zonation and characteristics of index forms. *University of Kansas Paleo Contr, 62,* 1–425.

Vail, P. R. (1987). Seismic stratigraphy interpretation procedure. In A. W. Bally (Ed.), *Atlas of seismic stratigraphy*, AAPG studies in Geology 27(1), 1–10.

Vail, P. R., Mitchum, R. M. Jr., & Thompson, S. (1977a). Seismic stratigraphy and global changes of sea-level, part-3: Relative changes of sea-level From costal onlap. In: C. E. Pyton (Ed.), *Seismic stratigraphy applications to hydrocarbon exploration* (pp. 63–82). AAPG, Special Memoir, 26.

Vail, P. R., Mitchum, R. M. Jr., & Thompson, S. (1977b). Seismic stratigraphy and global changes of sea-level, part-4: Global cycles of relative changes in sea-level. In: C. E. Pyton (Ed.), *Seismic stratigraphy applications to hydrocarbon exploration* (pp. 83–97). AAPG, Special Memoir, 26.

Vail, P. R., Mitchum, R. M. Jr., Todd, R. G., Widmier, J. M., Thompson, 3III., Sangree, J. B., Bubb, J. N., & Hatfeilid, W. G. (1977c). Seismic stratigraphy and global changes of sea level. In C. E. Payton (Ed.) *Seismic stratigraphy applications to hydrocarbon exploration* (pp. 49–212). AAPG Memoir 26.

Van Wagoner, J. C., Mitchum, R. M., Campion, K. M., & Rahmanian, V. D. (1990). Siliciclastic sequence stratigraphy in well logs, cores and outcrops; concepts for high resolution correlation of time and facies. Methods in exploration series (p 74). American Association of Petroleum Geologists.

Van Wagoner, J. C., Posamentier, H. W., Mitchum, R. M., Vail, P. R., Sarg, J. F., Loutit, T. S., & Hardenbol, J. (1988). An overview of the fundamentals of sequence stratigraphy and key definitions. In C. K. Wilgus, B. C. Hastings, C. Kendall, C. G. St, H. W. Posamentier, C. A. Ross, & J. C. Van Wagoner (Eds.), *Sea-level changes: An integrated approach Soc. Econ. Plaeo. and mineral* (pp. 39–45). Spec. Pub. 42.

Wade, B. S., Pearson, P. N., Beggren, W. A., & Palike, H. (2011). Review and revision of Cenozoic tropical planktonic foraminiferal biostratigraphy and calibration to the geomagnetic polarity and astronomical time scale. *Earth Science, 104,* 111–142.

Younes, A. I., & McClay, K. (2002). Development of accommodation zones in the Gulf of Suez-Red Sea rift, Egypt. *American Association of Petroleum Geologists Bulletin, 86,* 1003–1026.